

PUBLISHED VERSION

Ameen, Muhsin M.; Magi, Vinicio; Abraham, John [Flame dynamics in the lift-off region of diesel jets](#) Proceedings of the Australian Combustion Symposium, Perth, WA, 6-8 November 2013 / Mingming Zhu, Yu Ma, Yun Yu, Hari Vuthaluru, Zhezi Zhang and Dongke Zhang (eds.): pp.304-307

The copyright of the individual papers contained in this volume is retained and owned by the authors of the papers.

PERMISSIONS

<http://www.anz-combustioninstitute.org/local/papers/ACS2013-Conference-Proceedings.pdf>

Reproduction of the papers within this volume, such as by photocopying or storing in electronic form, is permitted, provided that each paper is properly referenced.

The copyright of the individual papers contained in this volume is retained and owned by the authors of the papers. Neither The Combustion Institute Australia & New Zealand Section nor the Editors possess the copyright of the individual papers.

Clarification of the above was received 12 May 2014 via email, from the Combustion Institute anz

12 May 2014

<http://hdl.handle.net/2440/82560>

Flame Dynamics in the Lift-Off Region of Diesel Jets

Muhsin M. Ameen^{1,*}

Vinicio Magi^{1,2}

John Abraham^{1,3}

¹ School of Mechanical Engineering, Purdue University, West Lafayette, IN 47907-2088, USA

² School of Engineering, University of Basilicata, 85100 Potenza, Italy

³ School of Mechanical Engineering, University of Adelaide, Adelaide, South Australia 5005, Australia

Abstract

In this work, the large eddy simulation (LES) technique is employed to computationally model a lifted jet flame at conditions representative of those encountered in diesel engines. An unsteady flamelet progress variable (UFPV) model is used for turbulence/chemistry interactions. In the model, a look-up table of reaction source terms is generated as a function of mixture fraction Z , stoichiometric scalar dissipation rate χ_{st} , and progress variable C_{st} by solving the unsteady flamelet equations. In the present study, the progress variable is defined based on the sum of the major combustion products. A 37-species reduced chemical reaction mechanism for n-heptane is used to generate the UFPV libraries. The results show that ignition initiates at multiple points in the mixing layer around the jet, towards the edges of the jet, where the mixture fraction is rich, and the strain rates are within the ignition limits. These ignition kernels grow in time and merge to form a continuous flame front. Lift-off height is determined by the minimum axial distance from the orifice below which the local scalar dissipation rate does not favor ignition.

Keywords: Lifted flames, Unsteady flamelet progress variable, Flame dynamics, Large-eddy simulation, Diesel jets.

1. Introduction

In recent years, it has been shown through experimental studies that flame lift-off in reacting diesel jets is related to soot concentration in the jets [1, 2]. The suggestion is that the higher the lift-off, the greater the mixing upstream of the lift-off height which results in lower soot formation downstream in the jet. If this is indeed the case, predicting lift-off in reacting diesel jets is important in the context of multidimensional modeling of the jets. Accurate modeling, however, requires an understanding of the physics of lift-off. Bajaj *et al.* [3] have shown that an unsteady flamelet progress-variable (UFPV) model implemented within a Reynolds-Averaged Navier-Stokes (RANS) framework can predict ensemble-averaged ignition delay and lift-off height. The prediction of soot and NO_x is, however, likely to be dependent on the highly transient nature of the reacting turbulent jet. Furthermore, large scale turbulent structures and unsteady effects (e.g. extinction, re-ignition, flame weakening) are likely to influence mixing and subsequently soot and NO_x formation. RANS simulations cannot predict these unsteady effects and large-eddy simulations (LES) are required.

In the present study, LES is carried out of a jet generated by injecting n-heptane vapor at 373 K into air at a temperature of 1000 K and a pressure of 40 bar with a velocity of 150 m/s (corresponding to $\text{Re}=250,000$) through an orifice diameter of 200 μm . The computational domain, and the subgrid models used to model the turbulence and turbulence-chemistry interactions are discussed next. Results and discussion follow. The paper will end with summary and conclusions.

2. Computational Model

The computations are performed in a three-dimensional domain (Fig. 1) which extends 150 diameters in the axial direction and 75 diameters in the radial direction. The computational grid consists of approximately 7.9 million grid points (350 x 150 x 150). The grid is stretched in both the axial and radial directions with the maximum resolution located along the jet centerline. The grid spacing in the axial direction varies from 0.25 jet diameters near the inlet boundary to 0.50 jet diameters near the outlet boundary, and the grid spacing in the radial direction varies from approximately 0.10 jet diameters at the jet axis to 1.70 jet diameters at the side boundaries. Except for the inlet boundary, all of the domain boundaries are implemented as subsonic non-reflecting outflow conditions. The implementation details of these boundary conditions are discussed in Abraham and Magi [4] and Anders *et al.* [5]. Due to the presence of the higher velocity, temperature, and density gradients, the Artificial Diffusivity Scheme (ADS) sub-grid scale model introduced by Kawai and Lele [6] is employed to obtain stable results.

The UFPV model described in the work of Bajaj *et al.* [3] is used as the turbulence-chemistry interaction model. n-Heptane is employed as the surrogate fuel as in the work of Bajaj *et al.* [3]. A 37-species chemical reaction mechanism developed by Peters *et al.* [7] is employed to generate the UFPV libraries. In the UFPV model, the reaction rates are tabulated as a function of three independent variables - mixture fraction Z , scalar dissipation rate χ_{st} , and the progress variable C . For the tabulation, 51 points are used in the Z coordinate, 10 points in χ_{st} coordinate and 21 points in the C coordinate.

* Corresponding author:

Email: mameen@purdue.edu

The accuracy of the resolution adopted has been assessed by refining the number of points and repeating the computations. Additional details about this modeling approach can be found in Bajaj [8] and Bajaj *et al.* [3].

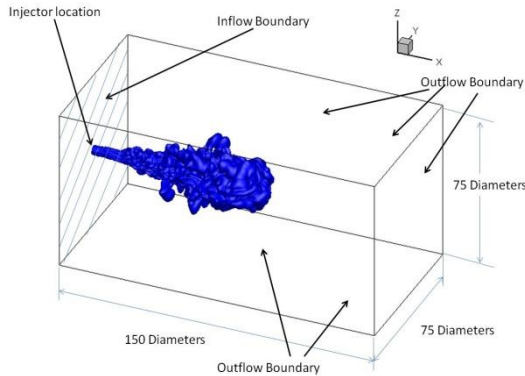


Figure 1. Computational domain and boundary conditions for LES

3. Results and Discussion

The LES of the jet was carried out until 1.0 ms after start of injection (ASI); the lift-off height reaches a steady value at approximately 0.65 ms. Figures 2 (a) - (c) show the transient evolution of the temperature in the central X-Y plane at three instants ASI. The different stages of ignition, flame development and flame stabilization are evident in these figures. It is found that the ignition delay is about 0.32 ms based on the criterion of when the temperature first reaches 1500 K. Figure 2 (a) shows temperature at 0.32 ms ASI. Ignition is noticeable at the leading edge of the jet. This ignition kernel grows with time. Meanwhile additional ignition kernels develop in the jet as can be seen in Fig. 2(b) which shows the temperature contours at 0.39 ms ASI. These ignition kernels develop spatially in time, and then merge to form a continuous flame (see Fig. 2 (c)). The lift-off height for this case is seen to be at the approximate axial distance of $x/D = 45$, i.e. 9 mm. There is no noticeable propagation of the flame upstream and the stabilization occurs at approximately the distance where the farthest upstream ignition occurs. Bajaj *et al.* [3] suggested by analyzing their RANS simulations that the lift-off height is at the location where the local scalar dissipation rate is equal to the ignition scalar dissipation rate. Examination of the scalar dissipation rate distribution in the results from these LES results show that the same mechanism is controlling in the LES.

Figure 3 shows the equivalence ratio-conditioned temperature averaged in the axial planes plotted as a function of the axial distance (only two equivalence ratios, 1.0 and 0.5, are shown). Figure 3 also shows that the temperature of 1500 K is reached at approximately $x/D = 45$. As expected the maximum temperature in the domain is observed in the stoichiometric mixture. Note that the temperatures in the stoichiometric mixture vary considerably depending on the strain rate and so the average temperature is noticeably lower than the corresponding adiabatic flame temperature.

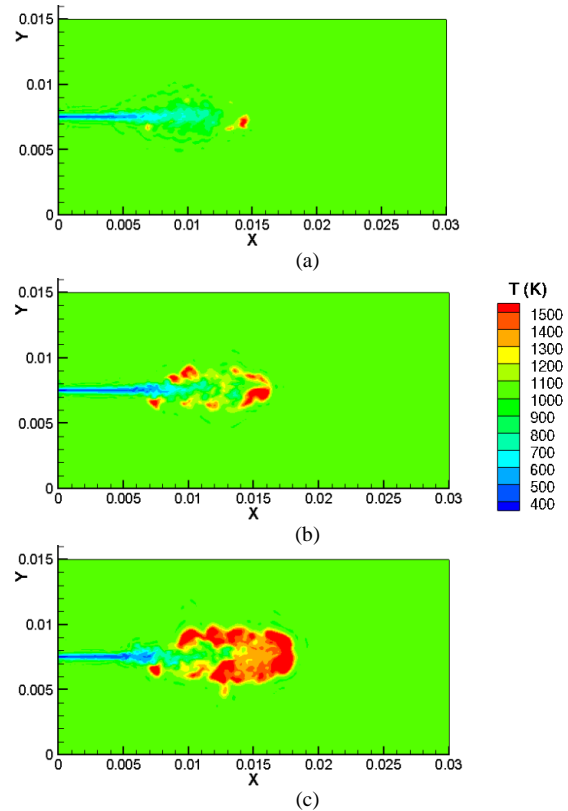


Figure 2. Transient evolution of the temperature in the central X-Y plane at (a) 0.32 ms, (b) 0.39 ms and (c) 0.50 ms ASI.

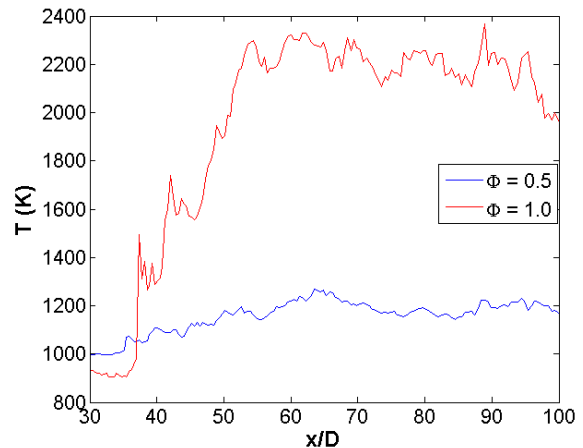


Figure 3: Variation of temperature conditioned with equivalence ratio as a function of the axial distance.

Understanding of these results often requires two-dimensional and three-dimensional views. This is especially important when drawing conclusions about local extinction. Figure 4 shows the flame surface in two different viewing orientations. The top row of figures show the low temperature contours (< 1500 K) in the central X-Y plane at 3 different time instants. At a time of 0.65 ms ASI, an ignition kernel can be seen at a location upstream of the lift-off height. As time progresses, this ignition kernel diminishes in size and is seen to be completely “extinguished” by the time of 0.75 ms. The second row of figures shows the temperature iso-surface of 1500 K at these same time instants, but now viewed from the X-Z plane. The circled part in these figures shows the location of the same ignition kernel. It can be now seen that the ignition kernel does

not actually extinguish but in fact rejoins the main flame front through a different plane. This development of the flame is seen to be in agreement with experimental observations of Takahashi and Goss [9] where local extinction is not visible upstream of the lift-off height. The bottom row of figures show the high-temperature contours (>1500 K). Significant variation in temperature can be seen. This was discussed earlier in relation to Fig. 3. This arises on account of the variations in scalar dissipation rate. The results show that the flame dynamics near the lift-off height is highly unsteady. The effect of such unsteadiness has been explored in prior studies [10, 11].

Figure 5 shows the velocity flow field near the lift-off height at two time instants. The left column shows the temperature contours and iso-lines of mixture fraction ($Z=0.05$ and $Z=0.08$), overlaid with the velocity vectors, and the right column shows the vorticity contours at the same physical time. Indirectly, these vorticity contours can be a measure of turbulence intensity. The vorticity values below $10,000$ s^{-1} are shown as the white region. It is seen that the maximum temperatures are observed in regions where the mixture fraction lies between 0.05 and 0.08. This is not surprising as the stoichiometric mixture fraction for n-

heptane is 0.062. It is also important to note that there are regions of the jet where the mixture fraction lies in this range but high-temperature reactions are not sustained because the strain rates in those regions are large. It can also be seen that the high temperature regions are located at regions where the vorticity are low ($< 15,000$ s^{-1}). The local turbulent flow field leads to the oscillation of the flame stabilization location about the nominally steady location of 9 mm (Figs. 5 (a) to (b)). The time-varying turbulent flow field near the flame stabilization location changes the structure of the flame with time. Another interesting aspect of this region is the presence of distinct large vortices at the flame stabilization location, as evident in Fig. 5. These vortices are not associated with large vorticity values but they can lead to large-scale mixing. Such vortices may play a role in stabilizing the flame as hypothesized by Broadwell *et al.* [12]. They hypothesized that flame stabilization occurs when hot gases, which have been convected to the edge of the jet by large-scale turbulent structures upstream of the plane of flame stabilization, are re-entrained and ignite non-combusting eddies of the jet [13]. If the mixing rate is too high, there is insufficient time for reactions to occur causing the gases to cool rapidly and ignition is prevented.

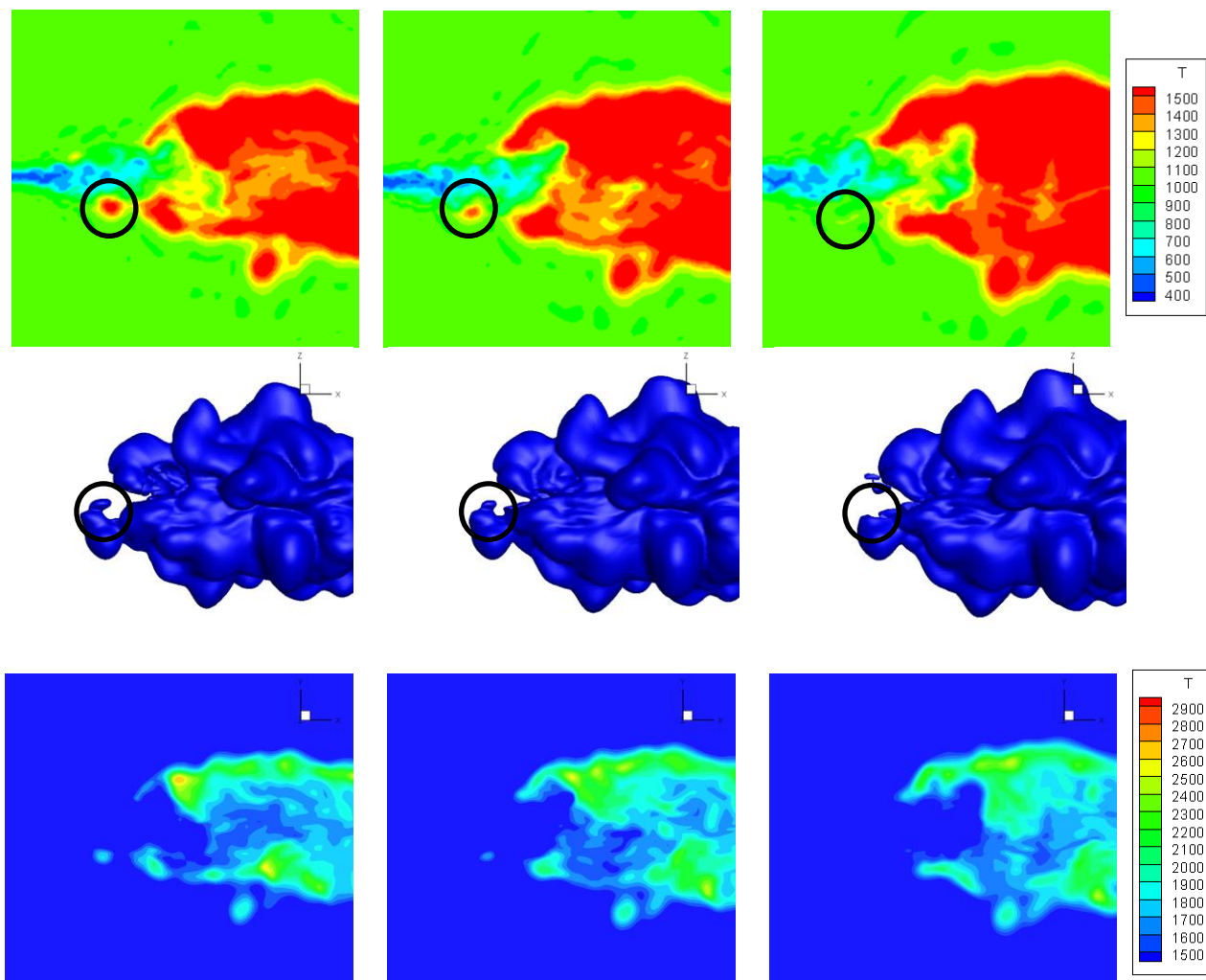


Figure 4: Transient evolution of flame upstream of the lift-off height at 0.65 ms, 0.70 ms and 0.75 ms. Top row: low temperature (<1500 K) contours in the XY plane; Middle row: temperature iso-surface (1500 K) shown from the XZ plane; Bottom row: high temperature (>1500 K) contours in the XY plane

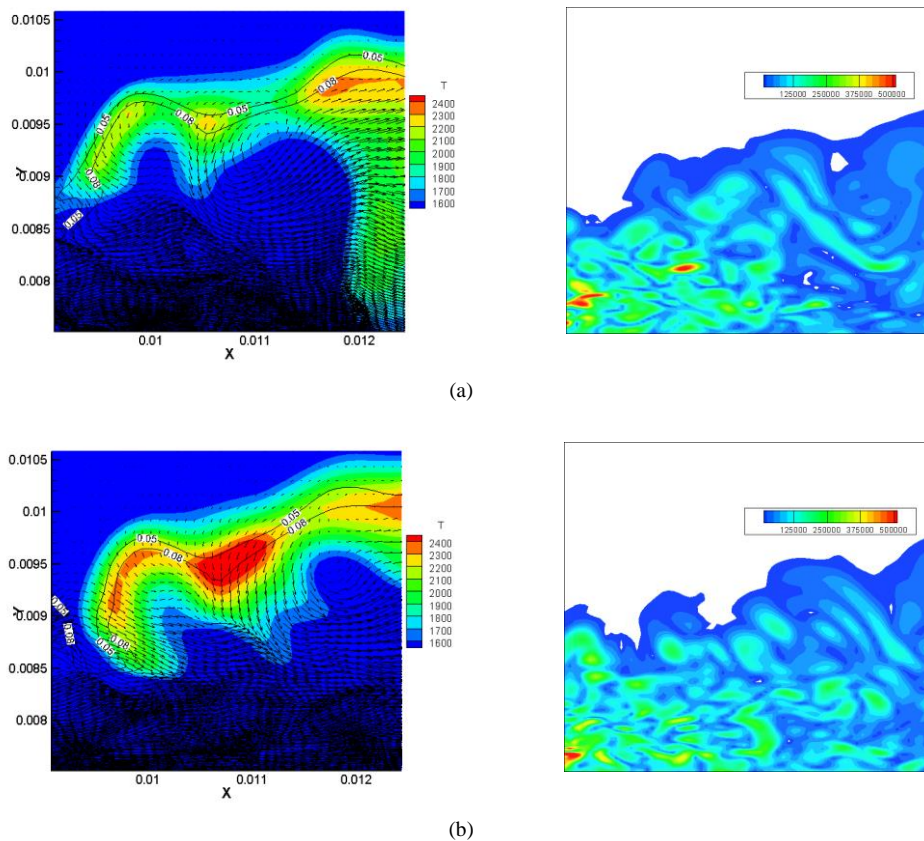


Figure 5: Flow field near the lift-off height at (a) 0.75 ms and (b) 0.80 ms ASI. The left column shows the temperature contours and the right column shows the vorticity contours. The dimensions on the axes are in m. Orifice diameter is 0.0002 m.

4. Conclusions

In the present study, LES of a lifted n-heptane turbulent reacting jet at high temperature and pressure conditions representative of those in diesel engines is performed. It is seen that ignition occurs at multiple locations along the edges of the jet. The ignition kernels grow in time and merge to form a continuous flame front. The lift-off height is determined by the minimum axial distance below which the local flow conditions do not favor the formation or growth of ignition kernels. The flame structure is seen to be highly unsteady, and affected strongly by the local flow-field. Large scale structures are observed near the lift-off height and it is possible that these structures can also lead to flame stabilization. This needs further study.

5. Acknowledgement

The authors would like to thank the National Institute of Computational Sciences (NICS), USA, and eResearch South Australia (eRSA) for providing the computing resources for this work. Financial support for this work was provided by Caterpillar, Inc.

6. References

- [1] D.L. Siebers, B.S. Higgins, SAE paper (2001) 2001-01-0530.
- [2] L.M. Pickett, D.L. Siebers, *Combust. Flame* 138 (2004) 114-135.
- [3] C. Bajaj, M.M. Ameen, J. Abraham, *Combust. Sci. Technol.* 185 (2013) 454-472.
- [4] J. Abraham, V. Magi *SAE Transactions* 106 (1997) 1442-1452.
- [5] J.W. Anders, V. Magi, J. Abraham, *Computers and Fluids* 36 (2007) 1609-1620.
- [6] S. Kawai, S.K. Lele, *J. Comput. Phys.* 227 (2008) 9498-9526.
- [7] N. Peters, G. Paczko, R. Seiser, K. Seshadri, *Combust. Flame* 128 (2002), 38-59.
- [8] C. Bajaj, MSME Thesis, Purdue University, West Lafayette, IN, 2012.
- [9] F Takahashi, L.P. Goss, 24th Symp. (Int.) Combust. 24 (1992) 351-359.
- [10] R Venugopal, J. Abraham, *AIAA J.* 47 (2009) 1491-1506.
- [11] R Venugopal, J. Abraham, *Combust. Sci. Tech.* 182 (2010) 717-738.
- [12] J.E. Broadwell, W.J.A. Dahm, M.G. Mungal, *Proc. Combust. Inst.*, 20 (1984) 303-311.
- [13] R. Venugopal, J. Abraham, SAE Paper 2007-01-0134, 2007.